# Design and Characterization of the Torsion Spring-Motor Integrated Series Elastic Actuator

Joonyoung Jang
Mechanical and Aerospace Engineering Department
University of California, San Diego
San Diego, USA
j7jang@ucsd.edu

Tao-Yi Wan

Mechanical and Aerospace Engineering Department University of California, San Diego San Diego, USA twan@ucsd.edu Zachary Hooker

Mechanical and Aerospace Engineering Department
University of California, San Diego
San Diego, USA
zhooker@ucsd.edu

Pablo Tejeda

Mechanical and Aerospace Engineering Department
University of California, San Diego
San Diego, USA
ptejeda@ucsd.edu

Thomas Bewley
Mechanical and Aerospace Engineering Department
University of California, San Diego
San Diego, USA
tbewley@ucsd.edu

Abstract—A Series Elastic Actuator (SEA) is a mechanical system that consists of a motor, an elastic material, and an end-effector placed in a series. By actuating the motor and loading the elastic material, the SEA can generate forces at the end-effector. Once the elastic material is loaded, the SEA can continuously produce forces without requiring additional motor actuation. This paper proposes a torsion spring-motor integrated SEA, specifically designed for applying consistent forces on a robot arm that can potentially contribute to achieving stability in robot poses. The SEA configuration comprises a motor securely attached to the body frame and a torsion spring connected between the robot arm and the motor shaft. When the robot arm contacts the ground, the actuating motor causes a deflection in the torsion spring. A force sensor positioned beneath the robot arm measures the pushing forces resulting from the deflection of the torsion spring. The torques can then be calculated by multiplying the distance between the SEA shaft and the robot arm by the measured force. Other design variations are also discussed with different assembly orders. The hardware tests show that the difference between the measured and estimated torques computed using Hooke's law of two suggested designs was an average of 0.0847 N-m and the normalized root mean square error of 13.48%.

Index Terms—Series Elastic Actuator, Torsion spring, Mechanical Design, Force sensor, Load cell

## I. INTRODUCTION

Actuators, such as servo or DC motors, have gained widespread usage in the field of robotics. Their reputation for reliability, precise position control, and resilience against external disturbances has spurred extensive research on their application in various domains. These include areas such as robot motion control, medical devices, compressors, and more [1]. However, these stiff actuators have inherent limitations

in dealing with unexpected forces caused by environmental impact or shock [2]. When subjected to large forces, the shaft or gearboxes of these actuators can be damaged. Furthermore, continuous motor actuation is required for robots that exert forces against the ground or a wall to maintain a stable pose.

Compared to stiff actuators, Series Elastic Actuators (SEAs) have built-in elastic materials, namely torsion springs. While traditional stiff actuators generate torques through electric current flow. SEA can derive torques from the deflection of an elastic material. The SEA is known for a complicated mechanism since it combines a motor, an elastic material, and structures depending on the configuration [3]. Despite its complexity, the SEA reduces the stiffness of conventional actuators and enables them to avoid unintended forces directly on motor parts. Leveraging this distinctive characteristic, SEAs can be effectively utilized as robot legs, as demonstrated by examples such as the Legged robot at MIT [4]. This enables the actuators to absorb unexpected shocks or disturbances resulting from impacts, enhancing the overall stability and resilience of the robot [5]. The benefits offered by SEAs have led to their widespread application in wearable robots and exoskeleton devices [6]. As the deflection of elastic materials determines the torque, SEAs also can be used as a force or torque sensor [7]. Additionally, the deflection of elastic materials allows SEAs to transmit force or torque to connected mechanisms without requiring additional motor actuation. Moreover, including elastic materials, such as springs, in SEAs transforms the force control problem into a position control problem, resulting in substantial improvements in force accuracy [8].

This paper focuses on exploring the feasibility of applying pushing forces on a robot arm. The proposed SEA aims to inherently obtain stability by passively expanding the robot across the full breadth of the wide range of narrow spaces, the springs firmly pressing the robot arms against opposite walls. Previous research has suggested various elastic components for SEAs, including compact and lightweight elastic beams [9], compression springs for linear motions [10], and torsion springs for rotational motions [11]. We propose the torsion spring-motor integrated SEA, as torque is required to push against the walls using the robot arm continuously. The motor is attached to the robot body frame or arm and driven to deflect the torsion spring. As the torsion spring deflects, torque is applied to the robot arm connected to the spring. Two different types of torsion spring-motor integrated SEAs were designed and tested for characterization. Also, to complement the limitation of two Types of SEAs, one conceptual design is suggested that can generate large torque using a DC motor for potential application in robots operating in various environments.

The paper is organized as follows. Section II presents the designs of the two suggested SEAs. Specifically, the first design, Type A, has a motor attached to the body frame, and the second design, Type B, has a motor attached to the robot arm. Both SEAs are designed for small-size robots operating in space-limited areas such as pipes. Section III explains the experimental setup, hardware components, and a customized force sensor calibration method in detail to measure the forces generated by the SEAs accurately. Section IV analyzes and discusses the experimental results, providing insights into the performance and characteristics of the proposed SEAs. Also, a larger torque model design, Type C, is suggested. Finally, Section V concludes the paper and outlines future directions for research.

## II. DESIGNS

This Section discusses two types of SEAs: Type A and Type B. These are designed explicitly for robots operating in confined spaces. A high-torque micro servo motor was utilized to simplify the design and achieve precise shaft angle control. Type A and Type B SEAs share the same hardware parts but they are connected in reverse order.

## A. Type A: Torsion Spring-Servo Integrated SEA

As shown in Fig. 1, Type A SEA features a servo motor mounted on the body frame, with Disk 2 attached to the servo motor hub. A D-profile shaft is rigidly connected with both Disk 1 and 2. Disk 1 links the shaft and torsion spring, enabling the transfer of motor torque to the spring. A torsion spring, securely attached to a robot arm, carries the torque from the servo motor and changes the arm angle. However, the arm angle remains constant when the robot arm comes into contact with the ground. Thus, as additional torque is applied to the spring by the servo motor, the torsion spring starts to deflect. It is highly suitable for constructing a robot arm that can apply continuous forces to walls or floors. The compact size of the Type A SEA is valuable for robots deployed in

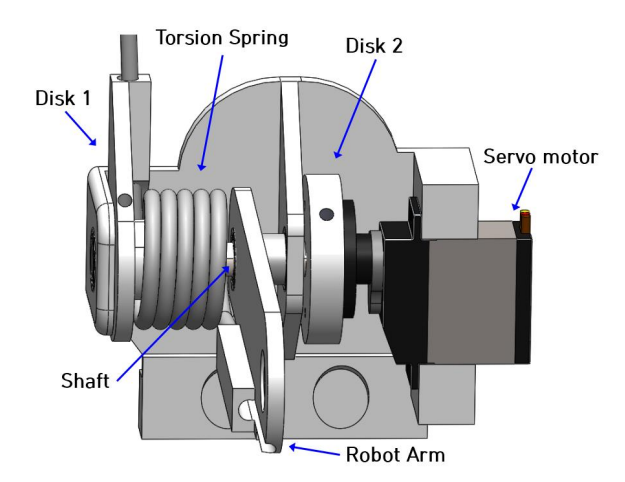


Fig. 1: Type A SEA: Consists of a servo motor, a torsion spring, a D-profile shaft, 3D printed disks, and a robot arm.

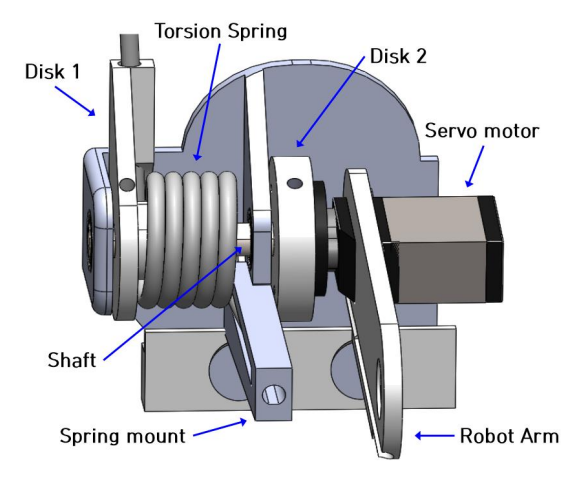


Fig. 2: Type B SEA: Parts are connected in reverse order compared to the Type A SEA.

narrow structures, allowing them to maintain their posture and stability. By leveraging the Type A SEA, these robots can effectively exert forces against the walls, ensuring their ability to navigate and operate within confined spaces.

## B. Type B: Reverse Torsion Spring-Servo Integrated SEA

Fig. 2 depicts the design of the Type B SEA, which is a variant of the Type A SEA sharing identical hardware components. However, the arrangement of these parts is reversed compared to the Type A SEA. A servo motor is embedded in a robot arm, and the servo motor hub is rigidly attached to Disk 2 and D profile links Disk 1 and Disk 2. As a torsion spring links Disk 1 and a spring mount on the body frame, the deflection of a torsion spring generates the pushing force on a robot arm. Since type B does not have servo motor mount on the body frame and have the smaller body width (Type A: 3.07', Type B: 2.65'), this design has benefits to fit inside the smaller space.

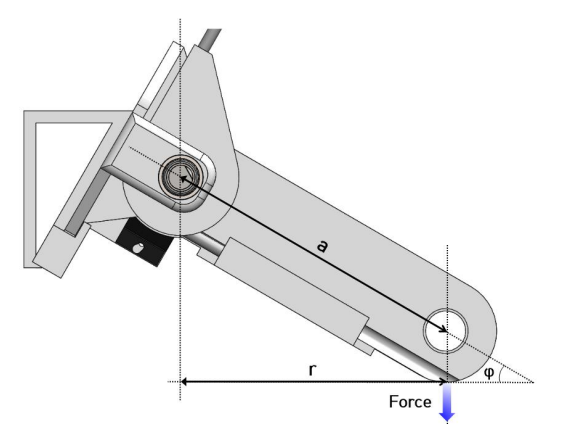


Fig. 3: Type A SEA Side View: a is the arm length, and  $\phi$  is the initial arm angle. r can be calculated as  $r = a \cos \phi$ . As the motor is actuated and the torsion spring is deflected, the force at the edge of a robot arm pushes against the ground.

### III. EXPERIMENT SETUP

The hardware parts details for the experiment are listed in TABLE I. The SEA contains a motor, a spring, and a robot arm connected in series. The experiment aims to measure the forces of suggested SEA designs to characterize them.

TABLE I: Hardware Parts

Category	Specification	
Motor (Stall torque)	RS100 Micro Servo (1.7037 N-m at 6V)	
Shaft	6mm D-profile	
Torsion Spring	Music wire steel (Max. torque 3.16 N-m)	
Microprocessor	Arduino Uno	
Force sensor	Load cell force sensor	

## A. Torsion Spring Torque

The torque  $\tau$  by a torsion spring can be calculated based on Hooke's law [12],

$$\tau = k \triangle \theta, \tag{1}$$

where k is the spring rate,  $\triangle \theta$  is the torsion spring deflection angle. The torsion spring rate k differs depending on the spring configuration and is determined by [13],

$$k = \frac{Ed^4}{64DN_a} \text{ (N-m/rad)}, \tag{2}$$

with E representing the modulus of elasticity, d wire diameter, D mean diameter, and  $N_a$  the number of active coils defined by following equation with the spring coil number N and the leg length L [14],

$$N_a = N + \frac{L}{3\pi d}$$

Leveraging torsion spring specifications listed in Table II, the spring rate of a torsion spring is 1.2005 N-m/rad. Meanwhile, the measured torques are obtained by gauging forces at the edge of robot arms and multiplying by the length between



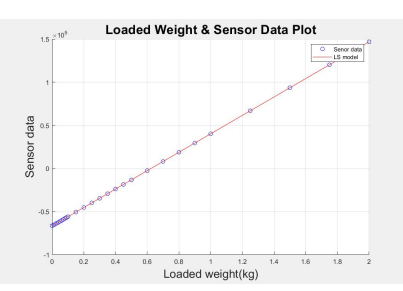


(a) Force Sensor

(b) Load Cell

Fig. 4: Customized force sensor utilizing a load cell.





(a) Calibration

(b) Force sensor calibration plot

Fig. 5: Calibrating the customized force sensor. Certain weights were added to the force sensor to obtain raw data. The plot shows the relationship between the loaded weight and the sensor's raw data. Blue circles are sensor data, and the solid red line is the LS model.

TABLE II: Torsion Spring Specification

Category	Specification
E (Modulus of elasticity, N/m <sup>2</sup> )	$2.0684 \times 10^{11}$
d (Wire diameter, m)	0.0029
D (Mean diameter, m)	0.0219
N (Number of coils)	5.25
L (Leg length, m)	0.1016

the SEA shaft and the shaft hole on the arm. Fig. 3 shows the side view of Type A SEA, and torque generated by SEA can be calculated by multiplying force f by the horizontal distance r. Then, the measured torque  $\tau_m$  is written as,

$$\tau_m = rf = \cos\phi f,\tag{3}$$

where  $\phi$  is the initial arm angle at which the robot arm makes contact with the ground, marking the beginning of spring deflection. This angle is measured by a protractor and is not assumed to be changing.

# B. Force Sensor

The torsion spring deflection creates the pushing force at the robot arm as described in III-A. For simplicity, instead of measuring the spring deflection angle, a force sensor can be used to calculate the measured torque using (3). As seen in Fig. 4a, a load cell force sensor was located underneath the robot

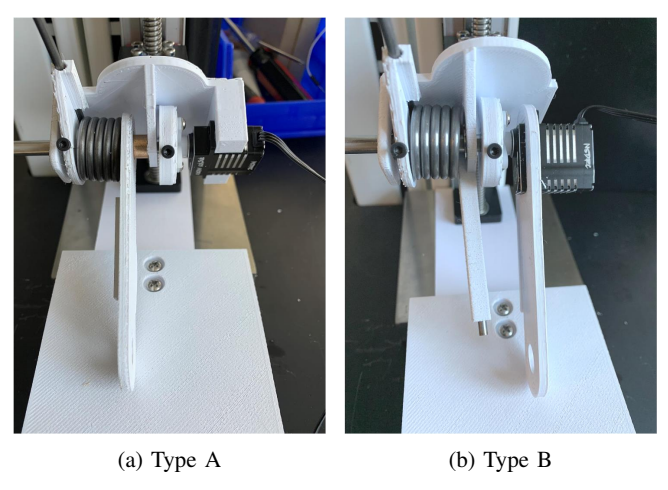


Fig. 6: Type A and B Hardware Model.

arm to measure the force. This customized force sensor uses a load cell seen in Fig. 4b. A load cell generates a voltage signal when the force is applied, and it is known that the output signal varies linearly with the load applied to the sensor [15] [16]. Thus, the Least Square (LS) method is suitable for calibrating a force sensor [17]. The linear relationship between the applied weight X and the load cell force sensor reading Y can be written as follows [18],

$$Y = aX + b, (4)$$

where (a, b) are parameters. Also, the sum of the error square with n numbers of data can be defined as,

$$\epsilon = \sum_{i=1}^{n} (Y_i - (aX_i + b))^2. \tag{5}$$

To find parameters (a, b) to minimize (5), take the derivative of (5) about a and b,

$$\frac{\delta\epsilon}{\delta a} = 2a \sum_{i=1}^{n} X_i^2 + 2b \sum_{i=1}^{n} X_i - 2 \sum_{i=1}^{n} X_i Y_i = 0,$$

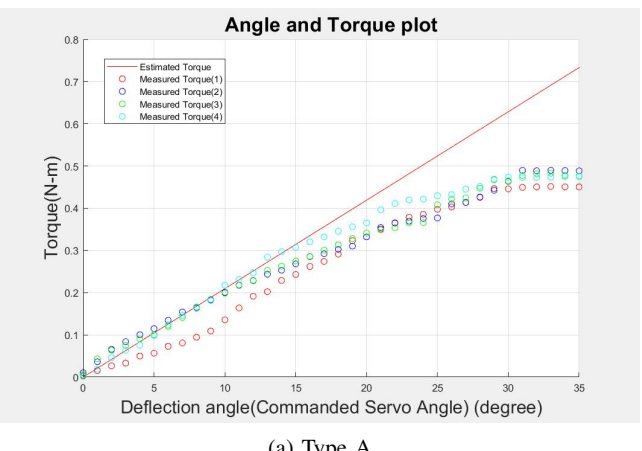
$$\frac{\delta\epsilon}{\delta b} = 2a \sum_{i=1}^{n} X_i + 2nb - 2 \sum_{i=1}^{n} Y_i = 0.$$
(6)

The parameters are computed by solving (6) and written as,

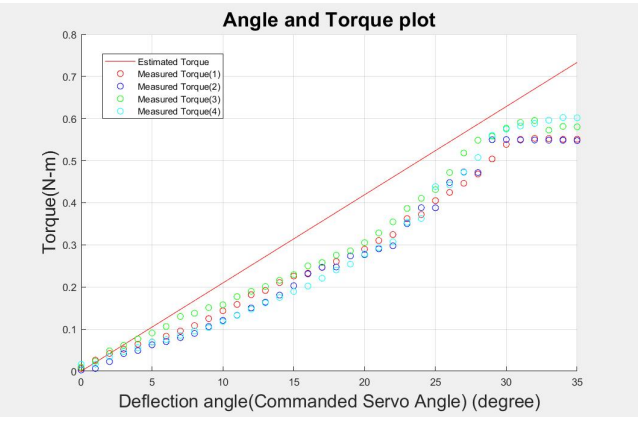
$$a = \frac{n \sum X_i Y_i - \sum X_i \sum Y_i}{n \sum X_i^2 - \sum X_i \sum X_i}$$

$$b = \frac{\sum Y_i - a \sum X_i}{n}.$$
(7)

As seen in Fig. 5a, the calibration was performed by adding certain weights to the force sensor. Sensor raw data were collected, and the LS model can be determined though  $(4)\sim(7)$ . The calculated parameters were  $a=1.0675\times 10^5, b=$  $-0.6662 \times 10^5$ , and Fig. 5b shows the sensor raw data and LS model. The LS model's Root Mean Square Error(RMSE) compared to the measured weight calculated from the sensor's raw data was  $2.0640 \times 10^{-4}$  kg, and the sensor raw data appears to be practically linear to the loaded weight.



(a) Type A



(b) Type B

Fig. 7: The relation between torsion spring deflection angle and the output torque of each SEA type. The deflection angle changes from 0 to 35 degrees, and four tests were performed for each model. Circles are  $torque(\tau_m)$  calculated by (3) about commanded servo motor torque, and the solid red line is estimated torque( $\tau$ ) computed by (1) about deflection angle.

## IV. EXPERIMENTAL RESULTS ANALYSIS

## A. Measured Torque Compared to Estimated Torque

Each SEA hardware test model was built as shown in Fig. 6. The experiment aims to measure the generated torque of proposed SEAs and analyze the error between the measured and estimated torque. The torque plots, shown in Fig. 7, illustrate the relationship between the deflection angle and torque. The measured torques of Type A and Type B in Fig. 7a, 7b demonstrate a nearly linear relation from 0 to 30 degrees of deflection angle, but it remains constant beyond 30 degrees. This observation can be attributed to the limited torque provided by the servo motor, which is insufficient to alter the angle of the torsion spring beyond a certain angle(30 degrees). Taking the data from 0 to 30 degrees deflection angle, the RMSEs and NRMSEs about estimated torques for each

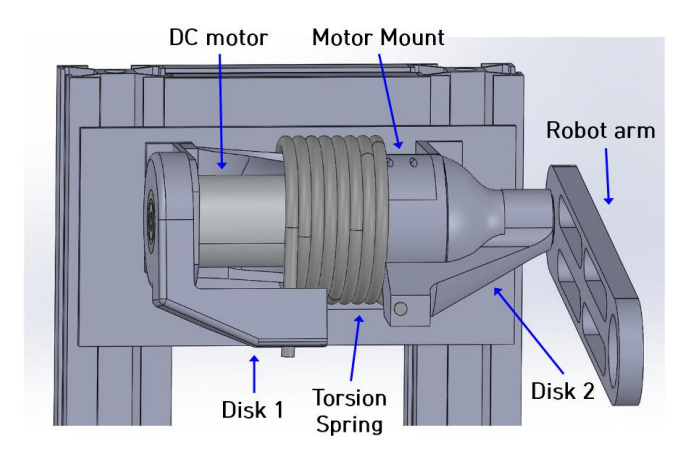


Fig. 8: Type C SEA: Consists of a high-torque DC motor, a customized torsion spring, 3D printed disks, and a robot arm.

type of SEA are as follows: Type A: 0.0797 N-m (12.68%), and Type B: 0.0897 N-m (14.28%). Note that the difference between the maximum and minimum values of the estimated torques was used as a scaler to normalize RMSE to calculate NRMSE. The average RMSE and NRMSE of both designs were 0.0847 N-m (13.48%).

## B. Possible Design for High-torque Requirement Robots

For heavy robots with many mechanical parts to cover large areas or perform multiple missions, we designed Type C, as shown in Fig. 8. Type C SEA is a larger size designed explicitly for high-torque-required robots. It incorporates a high-gear ratio DC motor with an encoder to generate the necessary torque. Type C SEA shares the same connection sequence of hardware parts as Type A SEA. However, the high-torque DC motor used in Type C allows for greater deflection of the torsion spring. The motor is positioned inside the torsion spring on the body frame to maintain a low-profile body width. The motor shaft is connected to Disk 1, which is linked to the torsion spring, and the other side of the torsion spring is connected to Disk 2. When the motor is actuated, the torsion starts to deflect, generating torque that applies a force to the robot arm connected to Disk 2. Considering the larger diameter of the torsion spring in Type C, selecting spring properties such as wire diameter and the number of coils is crucial to achieving the required spring rate defined as (2).

## V. CONCLUSION

This research proposes torsion spring-servo motor integrated SEAs that aim to generate continuous forces on a robot arm. These designs leverage the torsion spring's ability to generate torques through deflection, eliminating the need for constant motor actuation. The experimental results demonstrate that the output torques of both designs exhibit a nearly linear relationship with the deflection angle. Additionally, the CAD design of Model C, which employs a high-torque DC motor, is shown in Fig 8. This design is expected to provide greater deflection capabilities and is suitable for scenarios requiring

higher torque output and the capability of applying a feedback control model on robot arms as it uses a high-torque DC motor with an encoder.

Future work focuses on improving the hardware to reduce the potential sources of errors, particularly related to the use of low-cost 3D printed parts, such as disks. These parts may cause slip and result in torque loss from the servo motor. To mitigate this, it is required to replace these 3D printed components with more robust materials, such as metal, which can provide better reliability. Also, further tests and characterization of the Type C design are necessary, including constructing the hardware and conducting tests. In conclusion, this paper proposes different types of SEAs with unique characteristics, providing flexible solutions for accommodating various space constraints and torque demands on robotic applications.

## ACKNOWLEDGMENT

The authors gratefully acknowledge the financial support of the ERDC Construction Engineering Research Laboratory (CERL) via a subcontract with GTI Energy.

#### REFERENCES

- S. Mondal, A. Nandi, I. Mallick, C. Ghosh and A. Giri, "Performance evaluation of brushless DC motor drive for three different types of MOSFET based DC-DC converters," 2017 Devices for Integrated Circuit (DevIC), Kalyani, India, 2017, pp. 589-593, doi: 10.1109/DE-VIC.2017.8074019.
- [2] K. D. Truong, A. K. L. Luu, N. P. Tong, V. T. Duong, H. H. Nguyen and T. T. Nguyen, "Design of Series Elastic Actuator Applied for Humanoid," 2020 International Conference on Advanced Mechatronic Systems (ICAMechS), Hanoi, Vietnam, 2020, pp. 23-28, doi: 10.1109/ICAMechS49982.2020.9310118.
- [3] C. Lee, S. Kwak, J. Kwak, S. Oh, "Generalization of Series Elastic Actuator Configurations and Dynamic Behavior Comparison," Actuators 6, no. 3, 2017, https://doi.org/10.3390/act6030026.
- [4] G. Pratt, "Legged robots at MIT: what's new since Raibert?," IEEE Robotics & Automation Magazine, vol. 7, no. 3, pp. 15 – 19, 2000.
- [5] F. Sergi, D. Accoto, G. Carpino, N. L. Tagliamonte and E. Guglielmelli, "Design and characterization of a compact rotary Series Elastic Actuator for knee assistance during overground walking," 2012 4th IEEE RAS & EMBS International Conference on Biomedical Robotics and Biomechatronics (BioRob), Rome, Italy, 2012, pp. 1931-1936, doi: 10.1109/BioRob.2012.6290271.
- [6] E. J. Rouse, L. M. Mooney, E. C. Martinez-Villalpando and H. M. Herr, "Clutchable series-elastic actuator: Design of a robotic knee prosthesis for minimum energy consumption," 2013 IEEE 13th International Conference on Rehabilitation Robotics (ICORR), Seattle, WA, USA, 2013, pp. 1-6, doi: 10.1109/ICORR.2013.6650383.
- [7] A. Zibafar, S. Ghaffari and G. Vossoughi, "Achieving transparency in series elastic actuator of sharif lower limb exoskeleton using LLNF-NARX model," 2016 4th International Conference on Robotics and Mechatronics (ICROM), Tehran, Iran, 2016, pp. 398-403, doi: 10.1109/ICRoM.2016.7886771.
- [8] G. A. Pratt and M. M. Williamson, "Series elastic actuators," Proceedings 1995 IEEE/RSJ International Conference on Intelligent Robots and Systems. Human Robot Interaction and Cooperative Robots, Pittsburgh, PA, USA, 1995, pp. 399-406 vol.1, doi: 10.1109/IROS.1995.525827.
- [9] X. Yang, W. Luo, H. Liu, S. Zhang and W. Ge, "Optimal Design for the Torsional Elastic Element Topology of a Rotary Series Elastic Actuator," 2022 7th Asia-Pacific Conference on Intelligent Robot Systems (ACIRS), Tianjin, China, 2022, pp. 13-17, doi: 10.1109/ACIRS55390.2022.9845652.

- [10] D. W. Robinson, J. E. Pratt, D. J. Paluska and G. A. Pratt, "Series elastic actuator development for a biomimetic walking robot," 1999 IEEE/ASME International Conference on Advanced Intelligent Mechatronics (Cat. No.99TH8399), Atlanta, GA, USA, 1999, pp. 561-568, doi: 10.1109/AIM.1999.803231.
- [11] X. Qu, D. Cao, Q. Wang and Y. Li, "Design and Research of Flexible Joint with Variable Stiffness Based on Torsion Spring," 2019 IEEE International Conference on Mechatronics and Automation (ICMA), Tianjin, China, 2019, pp. 325-329, doi: 10.1109/ICMA.2019.8816529.
- [12] E. Campbell et al., "Design of a low-cost series elastic actuator for multirobot manipulation," 2011 IEEE International Conference on Robotics and Automation, 2011, pp. 5395–5400.
- [13] T. Hoeltgebaum, R. Luft, J. Elisii and R. Vieira, "A Design Comparison between Coil Springs and Torsion Bars," SAE Technical Paper 2012-36-0172, 2012, doi: 10.4271/2012-36-0172.
- [14] An Sei Metaltek Company (n.d.). Torsion Spring Key Parameters and Reference Numbers. Spring Engineers. Retrieved June 20, 2023, from https://www.springhouston.com/products/torsion-springs/keyparameters-/reference-numbers.html
- [15] S. Jaiteh, S. F. Adillah Suhaimi, T. Ching Seong, A. M. Buhari, L. Lini and H. Neyaz, "Smart Scale Tracking System Using Calibrated Load Cells," 2019 IEEE Conference on Sustainable Utilization and Development in Engineering and Technologies (CSUDET), Penang, Malaysia, 2019, pp. 170-174, doi: 10.1109/CSUDET47057.2019.9214692.
- [16] Nasir K., Shauri R. L. A. and Jaafar J., "Calibration of embedded force sensor for robotic hand manipulation," 2016 IEEE 12th International Colloquium on Signal Processing & Its Applications (CSPA), Melaka, Malaysia, 2016, pp. 351-355, doi: 10.1109/CSPA.2016.7515859.
- [17] M. Sharifzadeh, M. T. Masouleh and A. Kalhor, "Design, construction & calibration of a novel Human-Robot Interaction 3-DOF force sensor," 2015 3rd RSI International Conference on Robotics and Mechatronics (ICROM), Tehran, Iran, 2015, pp. 182-187, doi: 10.1109/ICROM.2015.7367781.
- [18] T. Nakano, K. Nagata, M. Yamada and K. Magatani, "Application of least square method for muscular strength estimation in hand motion recognition using surface EMG," 2009 Annual International Conference of the IEEE Engineering in Medicine and Biology Society, Minneapolis, MN, USA, 2009, pp. 2655-2658, doi: 10.1109/IEMBS.2009.5332858.